

## Review article

## Open Access

Jacob Scheuer\*

# Metasurfaces-based holography and beam shaping: engineering the phase profile of light

DOI 10.1515/nanoph-2016-0109

Received February 29, 2016; revised April 20, 2016; accepted May 8, 2016

**Abstract:** The ability to engineer and shape the phase profile of optical beams is in the heart of any optical element. Be it a simple lens or a sophisticated holographic element, the functionality of such components is dictated by their spatial phase response. In contrast to conventional optical components which rely on thickness variation to induce a phase profile, metasurfaces facilitate the realization of arbitrary phase distributions using large arrays with sub-wavelength and ultrathin (tens of nanometers) features. Such components can be easily realized using a single lithographic step and is highly suited for patterning a variety of substrates, including nonplanar and soft surfaces. In this article, we review the recent developments, potential, and opportunities of metasurfaces applications. We focus primarily on flat optical devices, holography, and beam-shaping applications as these are the key ingredients needed for the development of a new generation of optical devices which could find widespread applications in photonics.

**Keywords:** metasurfaces; plasmonics; flat optics; nano antennas; holography.

## 1 Introduction

The propagation of a beam of light can be determined completely by its phase and amplitude profiles at a given two-dimensional surface. This rule, which is related directly to the Huygens' principle [1] is one of the key tools for analyzing the properties of optical beams [2]. Moreover, the same principle can be applied in order to control and engineer the properties of such beams, and generate arbitrary profiles, simply by inducing a properly designed amplitude

and phase profile over conventional (e.g. plane wave or Gaussian shaped) beams.

Although complete control over the beam properties requires both amplitude and phase manipulation, much effort was focused on phase control in order to avoid undesired loss of optical power which leads to low efficiency [2]. Basic optical elements such as lenses, prisms, and mirrors, for example, are essentially phase-only elements which manipulate the propagation of optical beams by inducing upon them specific phase profiles. Phase-only manipulation is, therefore, a powerful tool which facilitates almost arbitrarily beam shaping by introducing a phase mask which can be designed by a variety of numerical algorithms such as the Gerchberg-Saxton (GS) algorithm and its derivatives [3, 4].

In this article, the recent developments in metasurfaces-based phase control and engineering approaches, as well as their applications for holography and beam shaping, are reviewed. Metasurfaces are planar structures which can modulate the local properties (amplitude, phase, polarization, etc.) of an optical beam which is reflected from or transmitted through them [5–10]. Metasurfaces consist of large arrays of metallic or dielectric nano-structures which scatter the impinging light. The shape and dimensions of these nano-structures determine the phase (and amplitude) at which the light is scattered from them, thus facilitating full control over the phase (and amplitude) profile of the beam which emerges from the metasurface [5, 11–15].

The ability of metasurfaces to provide high-resolution control over the phase profile of optical beam, render them very attractive for many applications but in particular for holography and beam shaping [16–30]. Indeed, studies on metasurfaces-based holography and beam shaping (primarily at mid and far IR) begun emerging more than a decade ago [11, 12, 31] where recent studies utilizing metallic and dielectric nano-structure demonstrated devices for short-IR and visible [5, 20].

The rest of this article is arranged as follows: In Section 2 we briefly review the properties of metasurfaces and their design strategies and in Section 3 we present their

\*Corresponding author: Jacob Scheuer, School of Electrical Engineering, Tel-Aviv University, Ramat-Aviv, Tel-Aviv 69978, Israel, e-mail: kobys@eng.tau.ac.il

physical implementations. In Section 4 we review the limitation, hurdles, and challenges in realizing metasurfaces-based devices and in Section 5 we summarize and conclude.

## 2 The basics of metasurfaces

As mentioned in Section 1, metasurfaces consist of array of sub-wavelength nano-structures which can be considered as the pixels of a phase (and, in general, amplitude) mask. The main idea is shown in Figure 1: a flat surface is divided into discrete pixels where each pixel provides a specific, local, phase shift indicated by  $\phi_{ij}$  which represents a discretized version of a phase map,  $\phi(x,y)$ .  $\phi(x,y)$  is the phase profile which is required for obtaining the desired beam shape.

After the incident beam is reflected from or transmitted through the metasurface and propagates a distance  $z$ , its field profile is given by the Kirchhoff integral:

$$U_z(x,y) = e^{i\frac{\pi}{\lambda z}(x^2+y^2)} \iint U_0(\xi,\eta) e^{i\frac{\pi}{\lambda z}(\xi^2+\eta^2) + i\phi(\xi,\eta)} \exp\left[-i\frac{2\pi}{\lambda z}(\xi x + \eta y)\right] d\xi d\eta \quad (1)$$

where  $U_0$  is the field profile of the impinging beam,  $\lambda$  is the wavelength, and  $U_z$  is the field profile at distance  $z$  from the metasurface. The design of a metasurface for beam shaping and holography applications exhibits two main challenges: (1) designing the appropriate phase mask needed for obtaining the desired beam shape; (2) designing the individual nano-structures needed for obtaining any desired phase shift between 0 and  $2\pi$  (i.e. the pixels).

### 2.1 Designing the phase profile

The simplest (and most common) type of hologram is the Fourier hologram which is designed to obtain the desired beam profile in the far field. Thus, the required mask is simply the inverse Fourier transform of the desired image [32]. However, this requires a phase and amplitude hologram which is more complex to fabricate but, more

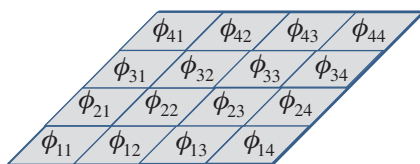


Figure 1: Schematic of a metasurface for phase control.

importantly, reduces the overall efficiency of the hologram defined as:

$$\eta = P_{\text{image}} / P_{\text{in}} \quad (2)$$

where  $P_{\text{image}}$  and  $P_{\text{in}}$  are the powers of the image and the input beams, respectively,

In order to improve the efficiency, it is desired to employ phase-only masks (or holograms). Nevertheless, the design and optimization of such mask are not trivial and often necessitates an iterative numeric approach. This is especially true if the mask is required to generate a complex pattern and not a simple functionality such as a beam deflector or lens whose phase pattern can be found analytically [5, 8–14, 22, 33]. As mentioned in the introduction, the most commonly employed approach for optimizing the phase mask is the GS algorithm [3, 4] which has proven to provide highly effective designs exhibiting efficiencies that exceed 80% [23–26].

The (practically) continuous phase map which is found either numerically or analytically must be quantized and discretized. Clearly, the choices of grid shape and resolution, and the number of quantization level have significant impact on the hologram efficiency, bandwidth, and fidelity [18, 23, 25, 34]. This point is further elaborated in Section 4 which deals with the limitations of metasurfaces-based holography.

### 2.2 Designing the individual pixels—the problem of spanning the $2\pi$ phase shift

Once the discrete and quantized phase map is obtained, it is necessary to construct a set of nano-structures (i.e. “pixels”) which can realize it. Probably the most important requirement from these nano-structures is the ability to span the complete  $2\pi$  shift needed to realize any arbitrary phase profile. One of the main difficulties in obtaining that property is that it requires nontrivial scatterers (or “nano-antennas”) because simple dipole antennas (which are the most commonly used elements) are inappropriate for this task. It should be noted that this statement is not entirely correct as dipole nano-antennas can be used in phase masks utilizing the concept of geometrical phase (or Pancharatnam–Berry phase as it is often referred to, as discussed in Section 3.3 below).

Figure 2 depicts the amplitude and phase responses of thin dipole antenna as a function of its length with respect to the impinging wavelength. The figure indicates two important issues that should be noted: (1) the phase response covers only up to a phase shift of  $\pi$ ; (2) the

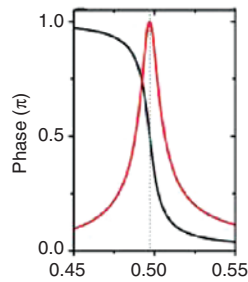


**Figure 2:** Phase (black) and amplitude (red) responses of a thin dipole nano-antenna. From Ref. [5]. Reprinted with permission from AAAS.

corresponding amplitude response decays substantially outside a narrow region around  $\pi/2$  phase shift. Thus, not only a straightforward implementation of thin dipole antennas cannot span the complete phase shift range, but also introduces a substantial amplitude response which impairs the efficiency of the hologram.

### 3 Implementations of metasurfaces for beam control

As mentioned earlier, the main challenge in utilizing metasurfaces for phase control and beam shaping is the ability to obtain any possible phase shift in the range  $\{0, 2\pi\}$  while maintaining uniform amplitude response. In order to meet these demands, several techniques, and approaches for realizing metasurfaces have been developed and demonstrated. These techniques utilize a variety of mechanisms, such as plasmonic and dielectric resonances, cross-polarization interactions, coupled nano-antennas, geometrical phase, etc.

#### 3.1 Metallic transmit-arrays

The works of Yu et al. [5] and Ni et al. [13] on phase control using V-shaped antennas is probably the most well-known (although not necessarily the first) demonstration of the potential of metasurfaces. V-shaped antennas have been known for decades and have been used in radio frequency (RF) communication links, TV sets and more. These antennas are relatively broad band and versatile and support two oscillation modes—a symmetric and an antisymmetric which differ in frequency by approximately a factor of two [35–37].

Figure 3 depicts a scanning electron microscopy image of the V-shaped antennas employed by Yu et al. [5]

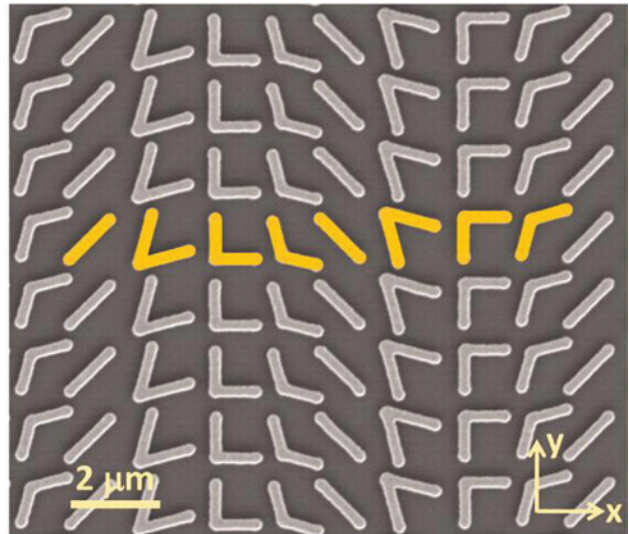


**Figure 3:** Metasurface utilizing V-shaped nanoantennas. From Ref. [5]. Reprinted with permission from AAAS.

at the far IR and later by Ni et al. [13] at the near IR, for inducing a phase gradient on a surface and modifying the refraction and reflection angles (i.e. realizing a deflector or an equivalent prism). The V-shaped antennas allow for needed  $2\pi$  phase shift control through polarization conversion. The specific phase response of each pixel is determined by the angle between the two arms of the antennas. The eight antennas marked in Figure 3 correspond to the unit cell of a deflector where each element provides a different phase shift which is a multiple of  $\pi/4$ .

One of the drawbacks of the V-shaped antennas implementation is that the phase shift is obtained through a polarization conversion mechanism. This requires the excitation of both modes of the nano-antennas and post-selecting only the component of the scattered field which is orthogonally polarized to the impinging beam. As a result the overall efficiency of the metasurface as defined in Eq. (1) is relatively low.

The V-shaped antennas are obviously not the only approach for spanning the necessary  $2\pi$  phase shift range. Other approaches such as patch antennas [24, 33, 38] have been shown to span the necessary range. However, these approaches have been demonstrated in the framework of reflect-arrays which are reviewed in Section 3.2 below. Nevertheless, it should be emphasized that the  $2\pi$  phase spanning obtained by the structure reported in Refs. [24, 33, 38] stem from using nondipole antennas and a reflective back plane.

The relatively low efficiency exhibited by plasmonic transmit-array stems not only from polarization conversion issues (which do not exist in patch antennas and geometrical phase based metasurface—see also

Section 3.3 below) but also from inherent properties of plasmonic scatterers. Plasmonic nano-antennas re-radiate (or scatter) the impinging light, more or less, homogeneously in all directions—including backwards. Consequently, a non-negligible part of the incident light is back reflected leading to low transmission efficiency.

Overcoming the efficiency problem require special arrangement such as multi-layer metasurfaces. More specifically, it has been shown that constructing a metasurface comprising three (or more) plasmonic layers can enhance substantially the transmission efficiency [39, 40]. Such metasurfaces have been demonstrated by several groups. Walther et al. demonstrated multi-layer fishnet-based hologram [16] and Larouche et al. realized a phase hologram consisting of several layers of I-beam inclusions [19]. Nevertheless, the fabrication of such metasurface is challenging, thus rendering the employment of this approach quite difficult. A recent alternative approach for reducing the back scattering, utilizes the properties of dielectric antennas, as discussed in Section 3.4.

Metallic transmit-arrays have been utilized for demonstrating several interesting applications. Flat optical lenses and deflectors (prisms) have been designed and realized experimentally [5, 13, 41, 42], as shown in

Figure 4. One of the attractive applications for such thin lenses is built-in collimators for solid-state lasers which facilitate lower divergence angle and enhanced beam quality [43–45]. In addition to conventional optical elements, more sophisticated devices such as quarter wavelength plate [46], vortex beams [14, 47] and circular vector beams [22, 48, 49] have been proposed and demonstrated experimentally.

Among the various applications of metasurfaces, holography is probably the “holy grail” of phase control and beam shaping as it requires custom-made design of arbitrary phase profiles. Metasurfaces provides the ability to realize the ultimate hologram as they support full control over the phase response at each pixel. Zhou et al. showed theoretically that V-shaped antennas can be used for holographic beam projection [21]. Ni et al. demonstrated a 3D beam shaping (i.e. a hologram) at the visible spectral region by patterning a 30-nm thick Au layer with V-shaped voids [20] and Huang et al. realized a hologram by using metasurfaces made of sub-wavelength metallic nanorods with spatially varying orientations [18]. This approach utilized geometrical phase shift which is further discussed in Section 3.3. A multi-layer metasurface hologram was demonstrated by Larouche et al. in the far IR

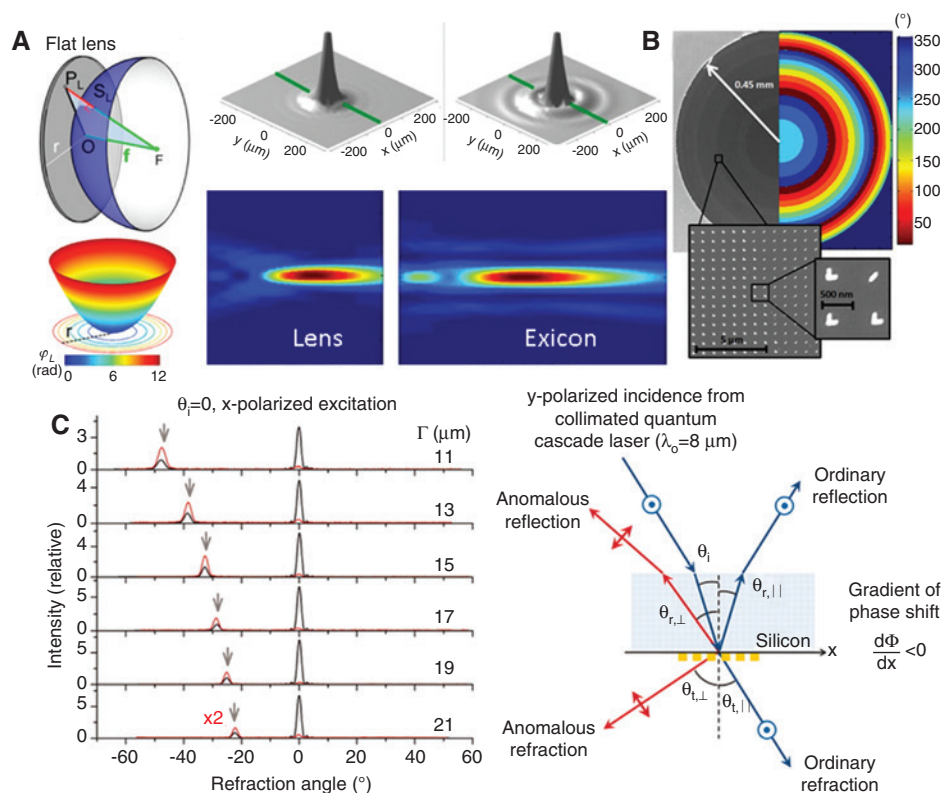


**Figure 4:** Plasmonic transmit arrays applications. (A); (B) Plasmonic metalenses. Adapted with permission from Ref. [41]. Copyright 2012 American Chemical Society; (C) plasmonic deflector/prism. From Ref. [5]. Reprinted with permission from AAAS.



spectral region [19]. This hologram included three vertically aligned metasurfaces where the phase map was composed of a mixture of metallic disks, rods, and I-shaped beams. More recently, Pfeiffer et al. demonstrated a beam deflector at telecom wavelengths by constructing vertically three metasurfaces consisting of combinations of apertures and disks [50].

### 3.2 Nano-antennas reflect-arrays

As mentioned in Section 3.1, transmit-arrays utilizing plasmonic nano-antennas exhibit relatively low efficiency which is inherent to their structure and can be overcome using complex multi-layer arrangements. An alternative approach is constructing a reflect-array metasurface by realizing a single layer metasurface over a reflective back-plane separated by a nonconductive transparent layer which is approximately  $\lambda/4$  thick [23–25, 33, 38, 51].

Reflect-arrays are a well-established field in RF and millimeter waves. Such an array usually consists of a number of (often identical) elements, fed in a desired phase distribution, in front of a flat, electrically large reflecting surface. The objective is to produce a unidirectional beam, increasing antenna gain and reducing radiation in unwanted directions. The individual elements are

most commonly half wave dipoles, although they sometimes contain parasitic elements as well as driven elements (Figures 5 and 6).

The higher efficiency which is inherent to the reflect-array concept, renders this approach highly attractive for many applications such as holography [17, 23, 25, 27, 52], flat optical elements [53, 54], etc. In addition, it was shown that such reflect-arrays support wide optical band (several hundreds of nanometers) both in the IR and the visible spectral range. As for their RF counterparts, the combination of high efficiency and broadband operation render reflect-array optical metasurfaces highly attractive for numerous “real-life” applications. Nevertheless, such devices are limited to operation in reflection mode and cannot replace refractive elements such as lenses, prisms, etc.

### 3.3 Geometrical phase metasurfaces

Geometrical phase metasurfaces utilize space-variant polarization manipulation of the incident field in order to induce local phase retardation. This type of phase retardation is essentially a Pancharatnam-Berry (PB) phase shift [55–57] which in some cases is an undesired effect but can be utilized for beam shaping. Although geometrical

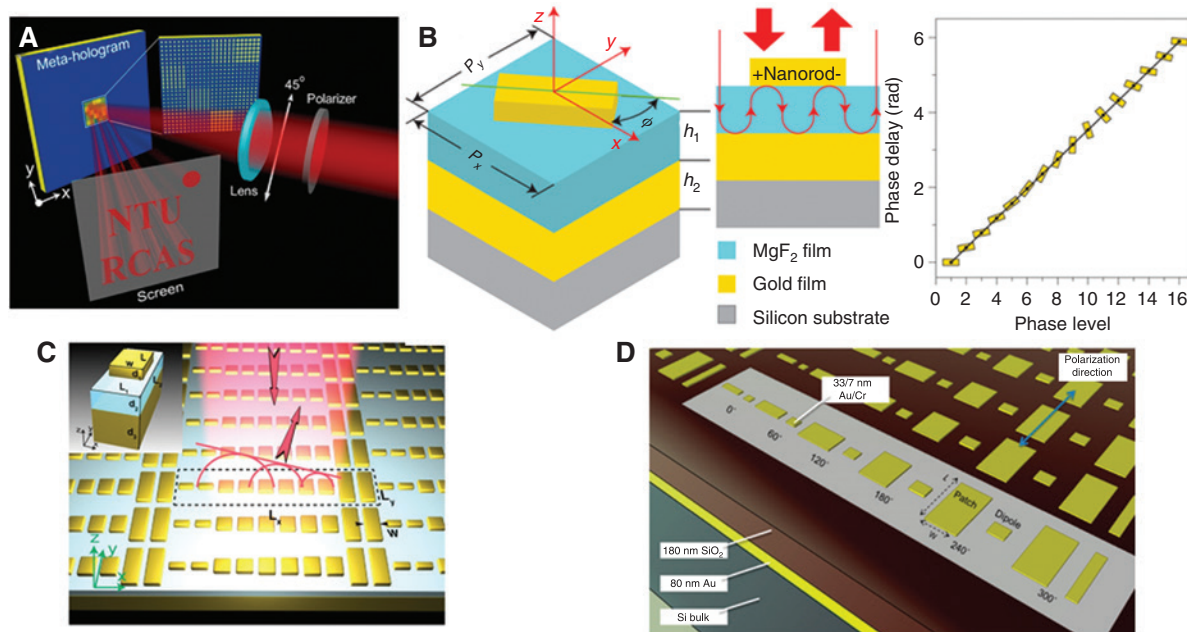


**Figure 5:** Plasmonic reflect-arrays. (A) Polarization control metasurface. Reprinted with permission from Ref. [24]. Copyright (2014) American Chemical Society; (B) geometrical phase reflect-array. Reprinted by permission from Macmillan Publishers Ltd: Nature Nanotechnology [25], copyright (2014); (C) reflective deflector. Reprinted with permission from Ref. [33]. Copyright (2012) American Chemical Society; (D) broadband reflective hologram. Reprinted with permission from Ref. [23]. Copyright (2014) American Chemical Society.

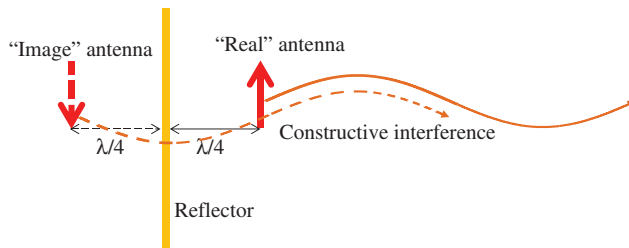


Figure 6: Enhanced efficiency of reflect-arrays.

phase metasurfaces can also be characterized as transmit/reflect-arrays as discussed in the previous sections, their unique properties as well as successful employment for highly efficient, broadband, holography merit special attention.

The concept behind geometrical phase control is simple. When a beam of circularly polarized (CP) light impinges upon an antenna with a linearly polarized resonance (e.g. a dipole), the scattered beam is partially converted into the opposite helicity with a phase shift which is determined solely by the geometrical orientation of the antenna [58–60]. Close to normal incident angles, a CP beam is primarily scattered into beams with identical polarization without phase change and to beams with the opposite circular polarization with a phase change corresponding to twice the angle formed between the dipole and a reference axis (note that precise normal incident this axis is arbitrary). The sign of the phase shift depends on the helicity state of the impinging beam (either right- or left-handed helicity). On the other hand, the amplitude of the scattered field is independent of the orientation of the antenna but rather on its frequency response.

The dependence of the phase retardation exclusively on the antenna orientation yields several inherent advantages of PB metasurface. Their response is very broadband, i.e. they can be used for inducing identical phase profile over a wide range of wavelengths. Their scattering efficiency (which determines the amplitude of the scattered wave) is determined by the properties of the specific type of antenna being used, which in the case of plasmonic antennas can quite broaden [61] and can even be designed to operate over more than an Octave [62].

Geometrical phase metasurfaces have been proposed and demonstrated as early as 2001 by the Hasman group using both metallic and dielectric nano-structures [11, 31, 63]. Using such metasurfaces, a variety of thin optical elements such as deflectors and complex beam-shapers have been demonstrated with remarkably high efficiencies. More recently the concepts of geometrical phase and deeply etched dielectric gratings were combined to realize

mode converters for circular vector beams [64] and highly efficient conventional and exicon lenses [65].

Geometrical phase metasurfaces have been shown to be highly attractive for both transmission and reflection holography. Zhang group has demonstrated a geometrical phase transmission hologram in the visible spectral range comprising Au nano-rods (i.e. dipole nano-antennas) [18]. More recently, the same group integrated their approach with a reflective backplane to demonstrate a highly efficient, wide angle and broadband reflection hologram [25], as well as dual-imaged helicity multiplexed reflection and transmission holograms [27].

It should be noted that although most of the recent studies involving geometrical phase metasurfaces utilized metallic nano-structures, the same approach can be extended to dielectric structures for beam shaping [31, 65] and for full color holography [30] and even to optically controlled materials such as linear photoalignment polymers and polymerizable liquid crystals [29]. This is yet another manifestation of the strength of the geometrical phase approach which does not rely on electronic/photon resonances but rather on polarization manipulation. It should be also noted that although most of the studies utilized polarization manipulation as means for phase control, it is also possible to combine them and obtain simultaneous phase and polarization control as was demonstrated by Yirmiyahu et al. [64] and more recently by Lin et al. [22]. This is, however, not trivial and requires special care as the two processes are not independent.

Finally, although geometrical phase is a powerful tool for holography and beam shaping application, this approach suffers from an inherent drawback—the impinging beam must be radially polarized. Although for some applications this is not a real concern, for others (such as authentication tags, where a source of CP light may not be immediately available) this limitation may prove crucial. Overcoming this constraint is not a trivial task as the mechanism of geometric phase is inherently linked with the properties of CP light.

### 3.4 Dielectric resonators

The integration of backplane reflectors with plasmonic metasurfaces facilitates the realization of reflective optical elements and holograms exhibiting impressive performances in terms of efficiency, bandwidth, and numerical aperture. Nevertheless, the reflect-array approach does not provide a means for realizing high-quality refractive elements (e.g. lenses, prisms, etc.) and beam shapers which necessitate transmit-arrays.

The two main drawbacks of metallic metasurfaces are their relatively low efficiency and sensitivity to polarization. And although polarization dependence might be acceptable or can even be a benefit for certain applications, low efficiency [as defined in Eq. (2)] is a major obstacle. Moreover, the low efficiency of plasmonic transmit-array is quite inherent to the properties of thin metallic scatters. When an electromagnetic wave is scattered from a metallic nano-particle, it primarily interacts with its electric dipole response. This response is relatively homogeneous in the horizontal plane leading to equal scattering in both forward and backward directions [66]. As a concrete example, consider an electromagnetic wave impinging upon a dipole antenna as shown in Figure 7. The impinging wave excites oscillating currents in the antenna leading to re-radiation of the energy towards all directions. Consequently, only a fraction of the impinging power is scattered towards the desired direction (forwards).

The efficiency problem can be partially resolved by employing several, vertically stacked, metasurfaces [19, 39, 40, 50] forming a Huygens' surface [1, 67, 68]. The underlying concept of a Huygens' surface is to excite properly phase-shifted electric and magnetic dipoles of equal amplitudes in order to obtain constructive interference in the forward direction and destructive interference in the backward direction. This condition is not satisfied by metallic nano-antennas as their magnetic dipole response is significantly smaller than that of their electric dipole. Vertically stacked metasurfaces, on the other hand, essentially obtain a similar condition by the mutual interference between the waves which are scattered by the layers.

In contrast to metallic nano-antennas, under certain conditions dielectric nano-particles possess a strong magnetic dipole response in addition to their electric one [69–75]. Specifically, it requires the optical thickness of the dielectric nano-structure to be of the order of half the

wavelength of the light in the material –  $W \approx \lambda/2n$ . Under this condition, the polarizations of the field in the edges of the nano-particle are opposite in direction, leading to the generation of a strong magnetic field at its center.

Having a strong magnetic dipole response is not enough. In order to obtain a preferred forward scattering of the impinging field it is necessary that the amplitude and phase of the magnetic and electric dipole responses are identical [69, 76]. Obtaining this requirement (often referred to as the first Krecker's condition) necessitates tailoring the geometrical dimensions of the nano-particle. In particular it is important to align the electric and magnetic resonances to the same wavelength not only for obtaining forward scattering over some optical bandwidth but for covering a complete  $2\pi$  phase shift.

Following the predictions and demonstration of magnetic resonances in dielectric nano-particles [71–73, 75–79], several groups have proposed and demonstrated dielectric metasurfaces for phase-control applications. Highly transmitting metasurfaces have been proposed by Cheng et al. [80] and have been demonstrated by Staude et al. using Si nano-disks [81]. Decker et al. [82], Shalaev et al. [83], and Yu et al. [84] utilized similar nano-structures to realize beam deflectors (i.e. prisms) in the IR and visible spectral regions, respectively. More sophisticated metasurfaces-based phase control such as an IR laser beam collimator was demonstrated recently by Arbabi et al. [85]. Lawrence et al. [86], Chong et al. [87] while Shalaev et al. [83] proposed and studied dielectric metasurfaces for vortex beam generation in the IR and the visible spectral regions. Note that unlike most studies in this field in which disk and elliptic shaped nano-structure are used, Shalaev et al. [83] employed arrays comprising rectangular dielectric resonators. We also note the work of Yang et al. [88] on vortex beam realization using dielectric resonators. Nevertheless, in this work, a reflect array was constructed where the phase control was obtained by

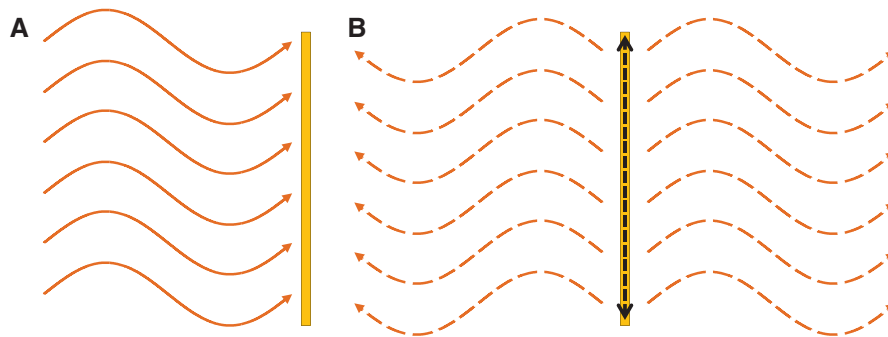


**Figure 7:** Re-radiation from a dipole antenna. (A) The antenna is excited by the incident wave; (B) The excited current re-radiates the energy forwards and backwards.

polarization conversion in a similar manner to the studies described in Section 3.3.

The research on both dielectric and plasmonic metasurfaces is primarily focused on obtaining a desired phase response while less consideration is given to the impact of the polarization state of the impinging and scattered fields. More specifically, most studies presented metasurfaces which exhibited polarization-dependent operation (though in some cases this was part of the metasurface functionality). While polarization independent dielectric metasurfaces have been demonstrated [87], a recent work by Arbabi et al. [89] demonstrated full control over both the phase profile and polarization state of the scattered field. The key idea in this study was to utilize elliptic-shaped dielectric resonators which were arranged in a hexagonal lattice. By controlling both the dimensions and orientation of the resonators, full control over the phase and polarization profile was obtained, thus facilitating efficient generation (more than 70%) of a variety of beams such as vortices and circular vector beams (CVBs), as well as the realization of flat lenses and holograms.

## 4 Hurdles and limitations of metasurfaces

The realization of any metasurface (either plasmonic or dielectric) requires several design and implementation steps—phase-map design, phase quantization, nano-antenna design, and fabrication. Each one of these stages eventually limits the overall performances of the device, primarily in terms of conversion efficiency.

### 4.1 Phase-map design

Given the desired profile of the scattering beam it is necessary to design an appropriate phase map which would convert the impinging power to the required beam in the most efficient way. In principle, the ideal mask can be obtained by inverting Eq. (1). However, this would result in a phase and amplitude mask which inherently blocks part of the incident power and limits the conversion efficiency.

Phase-only masks can provide a decent answer to the conversion efficiency problem but their design is often not obvious. Phase-only masks and holograms have been shown to yield very high efficiency for simple optical elements. This is, however, not surprising as such elements (such as lenses) induce only a phase profile on

the incident beam. Moreover, in many of these relatively simple cases the required phase map can be obtained analytically, leading to very high efficiencies [11, 12, 31, 33, 65]. On the other hand, obtaining the optimal phase mask for an arbitrarily shaped beam or for holography application is complex and necessitates iterative and sometimes stochastic algorithms [3, 4].

The very nature of these algorithms renders them sensitive to the initial condition (i.e. the initial “guess” for the phase map) which may lead to different final phase maps and conversion efficiencies. These algorithms ensure conversion of the phase map to a local minimum of the “cost” function (e.g. the deviation of the final image from the desired one) but not necessarily to the global minimum. Numerical studies on the efficiency penalty of the GS algorithm in the context of arbitrary beam shaping have shown that the expected penalty due to the design of the phase-map only is in the order of 20% [23]. Note that this penalty corresponds to an ideal courteous phase-map, i.e. before the quantization of the phase.

The design inefficiency is both image and algorithm dependent. It may vary between different target image, design algorithms, and the initial phase-map. In some cases it is useful to introduce a random “kick” to the phase map in order to try to converge to a better local minimum of the cost function. Nevertheless, this stochastic approach might also shift the solution to a worse minimum.

### 4.2 Phase quantization

A practical phase mask does not realize the phase map obtained from the design algorithm, but rather a discretized version consisting of a finite number of phase levels. The number of employed phase levels has a direct impact on the quality of the obtained image. In this context, metasurfaces employing various phase quantization levels, ranging between 4 and 16 have been realized and studied [5, 14, 18, 23–25, 33]. Nevertheless, little consideration was given to impact of the phase quantization. Yifat et al. studied the impact of the number of phase quantization levels on the conversion efficiency of phase metasurfaces, showing that the efficiency penalty of 6, 16, and 32 quantization levels is 20%, 10%, and 5%, respectively [23]. The exponential decrease of the penalty indicates that there is no practical reason to use more than 32 quantization levels. Moreover, developing a reliable process for fabricating nano-structures with such minute differences in order to obtain these small phase difference is extremely challenging, especially for the visible spectral region. Thus, it seems that 16–32 quantization levels are sufficient



to attain high quality representation of the continuous phase map obtained from the design process.

### 4.3 Pixel realization

Once the discretized and quantized phase map is obtained, it is necessary to assign to each pixel an appropriate nano-structure. This is by no means a simple task, particularly if a nonregular phase map is required.

The common approach to map the phase shift levels to a physical structure is to study (in most cases numerically) the spectral properties of the transmission and reflection of arrays comprising identical elements [5, 14, 33, 82, 87, 89]. The obtained phase (and amplitude) response is then associated with that of the individual element (i.e. pixel) in an arbitrary array (or hologram). In some of the realization approaches described earlier the phase-structure association is less complex. For example, the phase obtained by the pixels in geometrical phase based metasurfaces is determined simple by the orientation of the individual nano-structure.

The main difficulty with the approach described earlier is that it essentially neglects the coupling effects between the nano-structure comprising the metasurface.

It is well known from antenna theory that the presence of the adjacent elements in an array, effectively modifies the properties of the individual element [90]. Consequently, the phase response of each pixel in an arbitrary metasurface may differ substantially from its response in a homogeneous array [91], thus leading to errors in the realized phase-map.

The impact of these phase errors can be dramatic, especially in high-resolution metasurfaces, leading to significant reduction in the efficiency and to the formation of ghost images [92]. Ghost images are essentially the complex conjugated images of the desired object beam. The ghost image is projected to the opposite angle and is inverted with respect to the main image. In conventional holography, the power which is transferred to the ghost image is similar to that transferred to the desired image [32]. Metasurfaces, on the other hand, can modify and control the power transferred to the ghost image which can be theoretically eliminated completely. Figure 8 depicts examples of observed ghost images in metasurfaces-based holograms [23, 24]. Panel (B) of the figure depicts a simulation example for the appearance of a ghost image when small and random phase errors are added to an otherwise “perfect” hologram. Depending on the errors, the power directed to the ghost image could be quite significant. In

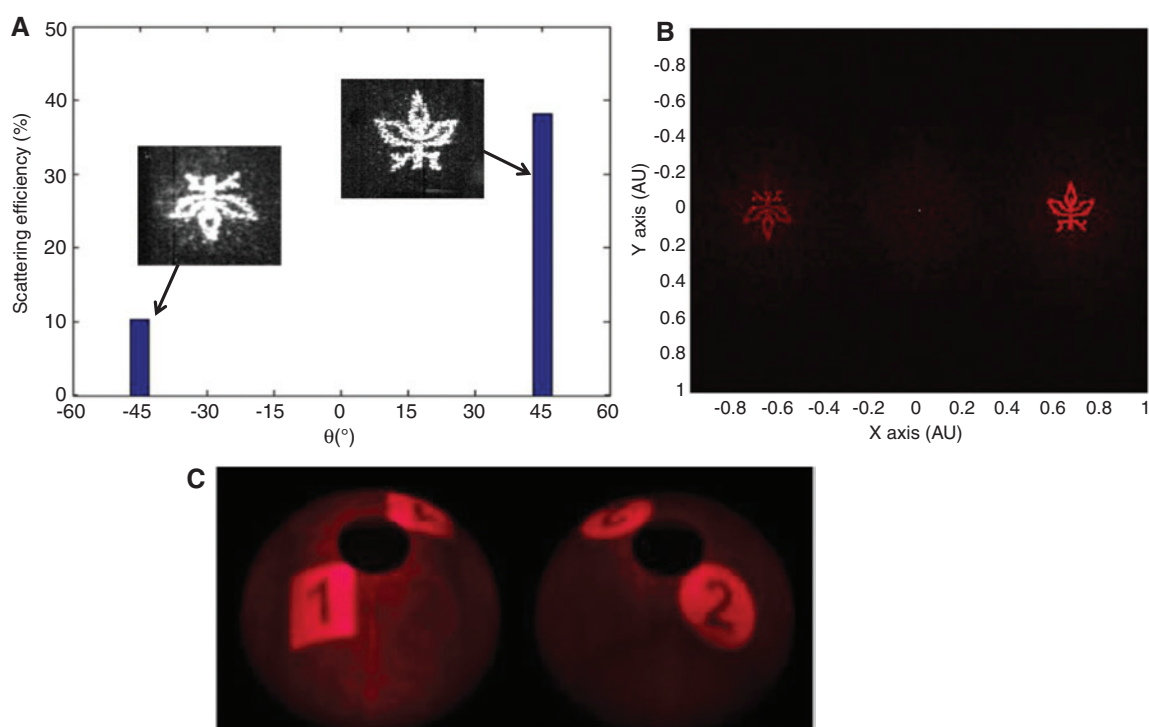


**Figure 8:** Ghost images in metasurface holograms: (A), (B) experimental observation and simulations. Adapted with permission from Ref. [23]. Copyright (2014) American Chemical Society; (C) experimental observation. Reprinted with permission from Ref. [52]. Copyright (2014) American Chemical Society.

the example shown in Figure 8 approximately 10% of the impinging power is directed to the ghost image.

It should be emphasized that the phase errors discussed in this Section do not stem from errors in the realization of the individual nano-structures but from the design approach for connecting between the pixel shape and its corresponding phase shift. The specific scatterer shape needed for obtaining a desired phase shift depends on its specific adjacent neighbors and, therefore, it is impossible to design a specific nano-antenna which yields a pre-determined phase shift.

In specific cases, such as deflect arrays and holograms design for large angle projections it is possible to partially overcome this problem by designing a supercell, consisting of several nano-antennas, which is intended for deflecting the light to the desired angle [33]. This approach takes into account the coupling between adjacent nano-antenna and can increase the efficiency substantially. Nevertheless, in an arbitrary phase profile metasurface, ideally each pixel should be designed according to its neighbors, which means that the whole hologram must be optimized simultaneously. Such optimization is obviously impractical and dealing with coupling effect still remains an open question.

Finally, it should be noted that the importance of the coupling effects may vary between the different metasurfaces realization approaches. For example, it was shown that coupling issues have relatively minor impact in geometrical phase and in dielectric resonators-based metasurfaces [25].

The geometrical phase approach is based on local manipulation of the polarization state which is obtained regardless of the resonance of the scattering nano-structure and radiation pattern. Consequently, one may expect that coupling effect between nano-antennas, which are likely to modify the spectral response, have less impact on the geometrical phase.

The weak coupling between dielectric resonators-based metasurfaces stem from the strong confinement of the resonating modes in the nano-structures and the relatively large separation between them [82]. As a result, the overlap between the modal fields of adjacent resonators is small and the corresponding impact on the phase response is relatively negligible.

#### 4.4 Fabrication tolerances and errors

The final step in the realization of a metasurface is the fabrication of the nano-structures composing the device. The development of the fabrication process requires

optimization of the employed lithography technique (most commonly E-beam) exposure value (dose) to ensure that the dimensions of the individual elements are as close as possible to the designed specifications. This optimization process introduces implicit assumptions on the structure of the array and, in particular, on the adjacent antennas surrounding the element being optimized. Consequently, the dimensions of some of the fabricated pixel may deviate from their desired ones, leading to phase errors.

The consequences of the phase errors due to fabrication tolerances are similar to those described in Section 4.3. However, as the source of the errors is not fundamental but rather technological, this effect can be mitigated to some extent by dynamically altering the dose for each element with regard to its neighbors.

## 5 Discussion, outlook, and challenges

The ability to use ultra-thin surfaces for shaping the amplitude, phase, and polarization profiles of optical beam by local manipulation of the electromagnetic field can open up new avenues for numerous applications in illumination, displays, integrated optics, power harvesting, virtual and augmented reality visors, and more. Such devices are expected to exhibit enhanced performances and functionality which can be readily realized using contemporary fabrication methods and can be integrated with electronics and peripheral components.

To date, a large part of the research involving metasurfaces is focused on the shaping and generation of unique beams (optical vortices, CVBs, etc.) and on holography. However, there is great potential in using metasurfaces for realizing future optical components such as aberration free and large numerical aperture lenses. Such technology can replace complex lenses consisting of multiple components by a simple and thin single surface [10, 41, 42, 93, 94]. Aberration correction using metasurfaces was recently demonstrated also in the context of electron microscopy where such problems are difficult to overcome [95].

Flat optical components are also highly attractive for integration with fiber optics and solid-state lasers as means for controlling the properties (divergence, polarization, etc.) of the output beam [44, 45, 96–103]. The ability to pattern fibers and lasers facets with corrective optics using conventional fabrication techniques such as focused ion beam and nano imprinting lithography paves the way to high-quality laser and light sources with numerous applications in communications, sensing, diagnostics, and therapy.

One of the important advantages of metasurfaces, especially plasmonic ones, is that their functionality is wavelength scalable and can be modified to fit a very wide range of frequencies. This is in contrast to dielectric materials whose properties are highly wavelength dependent. In particular, this property is advantageous for optical systems operating in the mid and far IR where refractive optical elements are based on special and often expensive materials. Metasurfaces-based optics is an attractive alternative approach at these spectral regions which are used by thermal imagers. In addition, metasurfaces can be utilized for modifying the spectral properties of thermal emitters [104, 105] with great potential for electric power generation from heat sources.

Another attractive property of metasurfaces stemming from their wavelength-dependent response is high-quality filters, especially in (but not limited to) the THz range [106–109]. The wavelength scaling property of metasurfaces facilitates their utilization over a wide spectral range, rendering them highly attractive for bands at which there are no good solutions.

Finally, the phase response of metasurfaces is naturally polarization dependent unless special care is taken. Although less attractive for some applications, such property is highly useful for many applications necessitating different processing of polarization states such as polarization convertors and analyzers [24, 46, 63, 110, 111], polarization multiplexing [24, 27, 28], etc.

Metasurfaces exhibit the ability to form and engineer the phase profile of a beam impinging upon it. Holography, flat optical components, and arbitrary beam shaping are probably the straightforward applications for such property but the potential of phase control with metasurfaces does not end here. Controlling the properties of beams generated by nonlinear processes is an emerging new application for such devices (see Ref. [112] and references therein). The combination of the strong nonlinear response that can be obtained from plasmonic nano-structure with the ability to control the phase properties of both the fundamental and higher harmonics can potentially initiate a new area of fundamental research and lead to the development of efficient, ultra-compact nonlinear optical devices [113–119].

Another interesting emerging application for phase engineering using metasurface is enhancing the interactions between light and charged particles. When a charged particle passes in the vicinity of metallic (or dielectric) periodic structure it radiates electromagnetic energy while losing part of its kinetic energy [120]. This process, generating the Smith-Purcell radiation, can be used for realizing electromagnetic radiations in a variety of wavelengths

[121, 122] and constitute the foundation for free electron lasers [123]. In addition, the reverse process where energy from light source is absorbed by a charged particle can be utilized to realize compact laser-driven accelerators [124, 125]. Plasmonic metasurfaces can further enhance the attainable acceleration gradient by utilizing both the plasmonic field enhancement and the ability to optimize the phase profile of the accelerating electric field [126]. Recent theoretical work has shown that metasurfaces laser driven accelerator can yield acceleration gradient exceeding 11 GV/m where the main limitation is the damage threshold of the materials being used [126].

Metasurfaces can be constructed using a variety of sub-wavelength structures—metallic nano-antennas, quantum dots, nano-particles, and dielectric nano-cavities. The ability to utilize them to induce arbitrary phase profile upon an impinging beam both in reflection and transmission opens up new avenues for numerous applications and exciting science. The next challenge of the research in this field is most likely the development of actively controlled and reconfigurable optical metasurfaces [127, 128], similar to phase-array antennas which are being widely used in the RF and millimeter waves regions. This challenge is considered by many as the “holy grail” of the research in metasurfaces. Having the ability to actively control phase fronts and beam profiles is a key to new and exciting applications such as laser radars, 3D holographic micro-projectors, tailored illumination for microscopy and many more.

The most straightforward approach for introducing tunability to optical metasurfaces is to exploit the sensitivity of plasmonic nano-antennas to their surrounding [129] by using materials which allow for modifying their refractive index. Such modification can be obtained by various mechanisms—thermal effects [130–132], electric and magnetic fields [133–143], liquid crystals (LC) [144], nonlinear optical effects [145, 146], mechanical strain [147–149], and free carriers injection [150]. Of particular great potential is the usage of phase changing materials (PCMs) which exhibit temperature-dependent transition from dielectric to metallic properties at room temperature [151–156]. Such transition is accompanied by substantial changes in the refractive index of the PCM, thus allowing for substantial shift in the resonance and phase response of nano-structures [152, 157].

Developing the ability to tune the resonance frequencies of nano-antennas is without doubt an important task. However, for beam-shaping and holography applications it is desired to be able to control the profile of the phase response of the array. Ideally, the phase response of each individual nano-antenna in the metasurface should be controlled separately. This is, in fact, one of the main challenges

in this field. Most of the studies involving dynamic metasurfaces were focused on either tuning the spectral response of the metasurface or on inducing relatively simple phase profile (e.g. linear phase gradient) [139, 152]. Few studies have demonstrated individual nano-antenna tuning but at relatively low frequencies [146] and limited spatial resolution using LC [144]. Optical tuning of individual nano-antenna in the near-IR spectral region was demonstrated by Abb et al. using free-carriers photo-generation in the indium tin oxide substrate with a 532 nm laser emitting 4ps pulses [150]. Nevertheless, the tuning effect was limited to several tens of ps due to the carriers' lifetime.

An alternative approach for light by light control with metasurfaces, utilizing coherent interference to control the scattering intensity (i.e. amplitude control) from each element in the array was recently demonstrated by Papaioannou et al. [158]. In this study, the interference between the control and signal beams was used for placing the peak or the node of the interference patterns at the position of a highly absorptive metasurface. Consequently, the amplitude profile of the signal beam can be controlled by modifying the properties of the control beam. This approach can obtain very fast (100 THz) switching and modulation speed rendering it highly attractive for various applications in imaging, telecommunications, and optical signal processing.

Long term (nonvolatile) tuning of surface optical properties was recently demonstrated by Zheludev's group [159]. The optical properties of chalcogenide glass PCM substrate (GST) were locally modified (written, erased, and rewritten) by inducing a refractive-index-changing phase transition with femtosecond pulses (see Figure 9). A similar approach can be readily employed to the tune

phase response of individual nano-antennas and to realize a completely reconfigure metasurface. It should be mentioned, however, that although such approach does yield high resolution arbitrary tuning of the phase profile, it is relatively slow and complex for some of the potential applications such as LIDAR, 3D projectors, etc.

The ability to arbitrarily shape the phase (as well as the amplitude and polarization) profile of light beam at sub-wavelength resolutions is a key and an enabling technology for numerous potential applications. With sufficiently high efficiency, polarization independence and tuning capabilities, such technology may prove to be the corner stone for not only lighter and more compact optical components but also for a completely new generation of optical devices and systems.

## References

- [1] Huygens C. *Traité de la Lumière* (Pieter van der Aa, Leyden, 1690).
- [2] Born M, Wolf E. *Principles of optics: electromagnetic theory of propagation, interference and diffraction of light*, 7<sup>th</sup> ed. New York, USA: Cambridge University Press, 1999.
- [3] Gerchberg RW, Saxton WO. A practical algorithm for the determination of phase from image and diffraction plane pictures. *Optik* 1972;35:237.
- [4] Fienup JR. Phase retrieval algorithms: a comparison. *Appl Opt* 1982;21:2758–69.
- [5] Yu N, Genevet P, Kats MA, Francesco A, Tetienne JP, Capasso F, Gaburro Z. Light propagation with phase discontinuities: generalized laws of reflection and refraction. *Science* 2011;334:333–7.
- [6] Holloway CL, Kuester EF, Gordon JA, O'Hara J, Booth J, Smith DR. An overview of the theory and applications of metasurfaces: the two dimensional equivalents of metamaterials. *IEEE Antennas Prop Mag* 2012;54:10–35.
- [7] Kats MA, Blanchard R, Patrice G, Capasso F. Nanometre optical coatings based on strong interference effects in highly absorbing media. *Nat Mater* 2013;12:20–4.
- [8] Kildishev AV, Boltasseva A, Shalaev VM. Planar photonics with metasurfaces. *Science* 2013;339:1232009.
- [9] Giovampaola CD, Engheta, N. Digital metamaterials. *Nat Mater* 2014;13:1115–21.
- [10] Yu N, Genevet P, Aieta F, Kats MA, Blanchard R, Aoust G, Tetienne JP, Gaburro Z, Capasso, F. Flat optics: controlling wavefronts with optical antenna metasurfaces. *IEEE J Sel Top Quant Electron* 2013;19:4700423.
- [11] Biener G, Niv A, Kleiner V, Hasman E. Formation of helical beams by use of Pancharatnam–Berry phase optical elements. *Opt Lett* 2002;21:1875–7.
- [12] Bomzon Z, Niv A, Kleiner V, Hasman E. Radially and azimuthally polarized beams generated by space-variant dielectric subwavelength gratings. *Opt Lett* 2002;5:285–7.
- [13] Ni X, Emani NK, Kildishev AV, Boltasseva A, Shalaev VM. Broad-band light bending with plasmonic nanoantennas. *Science* 2012;335:427.

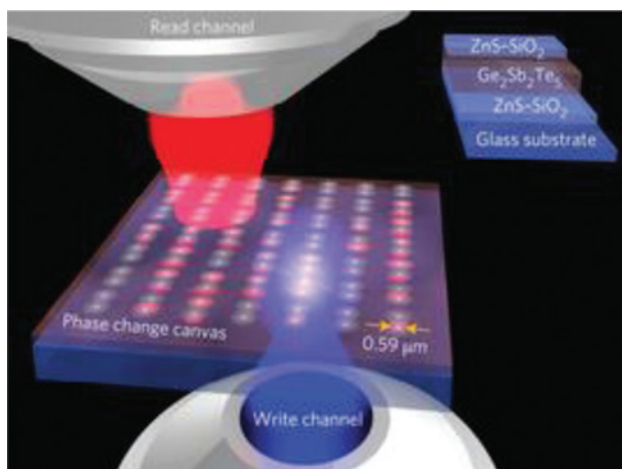


**Figure 9:** Reconfigurable metasurface consisting of a PCM substrate. Reprinted by permission from Macmillan Publishers Ltd: Nature Photonics [159], copyright (2016).



- [14] Genevet P, Yu N, Aieta F, Lin J, Kats MA, Blanchard R, Scully MO, Gaburro Z, Capasso F. Ultra-thin plasmonic optical vortex plate based on phase discontinuities. *Appl Phys Lett* 2012;100:013101.
- [15] Liu L, Zhang X, Kenney M, Su X, Xu N, Ouyang C, Shi Y, Han J, Zhang W, Zhang S. Broadband metasurfaces with simultaneous control of phase and amplitude. *Adv Mater* 2014;26:5031–6.
- [16] Walther B, Helgert C, Rockstuhl C, Setzpfandt F, Eilenberger F, Kley EB, Lederer F, Tünnermann A, Pertsch T. Spatial and spectral light shaping with metamaterials. *Adv Mater* 2012;24:6300–4.
- [17] Butt H, Montelongo Y, Butler T, Rajasekharan R, Dai Q, Shiva-Reddy SG, Wilkinson TD, Amaratunga AJ. Carbon nanotube based high resolution holograms. *Adv Mater* 2012;24:331–6.
- [18] Huang L, Chen X, Mühlenbernd H, Zhang H, Chen S, Bai B, Tan Q, Jin G, Cheah KW, Qiu CW, Li J, Zentgraf T, Zhang S. Three-dimensional optical holography using a plasmonic metasurface. *Nat Commun* 2013;4:2808.
- [19] Larouche S, Tsai YJ, Tyler T, Jokerst NM, Smith DR. Infrared metamaterial phase holograms. *Nat Mater* 2011;11:450–4.
- [20] Ni X, Kildishev AV, Shalaev VM. Metasurface holograms for visible light. *Nat Commun* 2013;4:2807.
- [21] Zhou F, Liu Y, Cai W. Plasmonic holographic imaging with V-shaped nanoantenna array. *Opt Express* 2013;21:4348–54.
- [22] Lin J, Genevet P, Kats MA, Antoniou N, Capasso F. Nanostructured holograms for broadband manipulation of vector beams. *Nano Lett* 2013;13:4269–74.
- [23] Yifat Y, Eitan M, Iluz Z, Hanein Y, Boag A, Scheuer J. Highly efficient and broadband wide-angle holography using patch-dipole nanoantenna reflect arrays. *Nano Lett* 2014;14:2485–90.
- [24] Chen WT, Yang KY, Wang CM, Huang YW, Sun G, Chiang ID, Liao CY, Hsu WL, Lin HT, Sun S, Zhou L, Liu AQ, Tsai DP. High-efficiency broadband meta-hologram with polarization-controlled dual images. *Nano Lett* 2014;14:225–30.
- [25] Zheng G, Mühlenbernd H, Kenney M, Li G, Zentgraf T, Zhang S. Metasurface holograms reaching 80% efficiency. *Nat Nano* 2014;10:308–12.
- [26] Scheuer J, Yifat Y. Holography: metasurfaces make it practical. *Nat Nano* 2015;10:296–8.
- [27] Wen D, Yue F, Li G, Zheng G, Chan K, Chen S, Chen M, Li KF, Wong PWH, Cheah KW, Pun EYB, Zhang S, Chen X. Helicity multiplexed broadband metasurface holograms. *Nat Commun* 2015;6:8241.
- [28] Wen D, Chen S, Yue F, Chan K, Chen M, Ardrón M, Li KF, Wong PWH, Cheah KW, Pun EYB, Li G, Zhang S, Chen X. Metasurface device with helicity-dependent functionality. *Adv Opt Mater* 2016;2:321–7.
- [29] Kim J, Li Y, Miskiewicz MN, Oh C, Kudenov MW, Escuti MJ. Fabrication of ideal geometric-phase holograms with arbitrary wavefronts. *Optica* 2015;2:958–64.
- [30] Zhao W, Liu B, Jiang H, Song J, Pei Y, Jiang Y. Full-color hologram using spatial multiplexing of dielectric metasurface. *Opt Lett* 2016;41:147–50.
- [31] Bomzon Z, Biener G, Kleiner V, Hasman E. Space-variant Pancharatnam–Berry phase optical elements with computer-generated subwavelength gratings. *Opt Lett* 2002;27:1141–3.
- [32] Goodman JW. Introduction to Fourier optics, 2<sup>nd</sup> ed. New York, USA: McGraw-Hill, 1998.
- [33] Sun S, Yang KY, Wang CM, Juan TK, Chen WT, Liao CY, He Q, Xiao S, Kung WT, Guo GY, Zhou L, Tsai DP. High-efficiency broadband anomalous reflection by gradient meta-surfaces. *Nano Lett* 2012;12:6223–9.
- [34] Egorov V, Eitan M, Scheuer J. High resolution efficient dielectric metasurface. *Lasers and Electro-Optics (CLEO), 2016 Conference on 5–10 June 2016, 2016*. pp. 1–2.
- [35] Svirko Y, Zheludev N, Osipov M. Layered chiral metallic microstructures with inductive coupling. *Appl Phys Lett* 2001;78:498–500.
- [36] Blanchard R, Aoust G, Genevet P, Yu N, Kats MA, Gaburro Z, Capasso F. Modeling nanoscale V-shaped antennas for the design of optical phased arrays. *Phys Rev B* 2012;85:155457.
- [37] Kats MA, Genevet P, Aoust G, Yu N, Blanchard R, Aieta F, Gaburro Z, Capasso F. Giant birefringence in optical antenna arrays with widely tailorable optical anisotropy. *Proc Natl Acad Sci USA* 2012;109:12364–8.
- [38] Sun S, He Q, Xiao S, Xu Q, Li X, Zhou L. Gradient-index metasurfaces as a bridge linking propagating waves and surface waves. *Nat Mater* 2011;11:426–31.
- [39] Monticone F, Estakhri NM, Alù A. Full control of nanoscale optical transmission with a composite metascreen. *Phys Rev Lett* 2013;110:203903.
- [40] Pfeiffer C, Grbic A. Metamaterial Huygens’ surfaces: tailoring wave fronts with reflectionless sheets. *Phys Rev Lett* 2013;110:197401.
- [41] Aieta F, Genevet P, Kats MA, Yu N, Blanchard R, Gaburro Z, Capasso F. Aberration-free ultra-thin flat lenses and axicons at telecom wavelengths based on plasmonic metasurfaces. *Nano Lett* 2012;12:4932–6.
- [42] Aieta F, Genevet P, Kats M, Capasso F. Aberrations of flat lenses and aplanatic metasurfaces. *Opt Express* 2013;21:31530.
- [43] Memarzadeh B, Mosallaei H. Array of planar plasmonic scatterers functioning as light concentrator. *Opt Lett* 2011;36:2569–71.
- [44] Yu N, Blanchard R, Fan J, Edamura T, Yamanishi M, Kan H, Capasso F. Small divergence semiconductor lasers with two-dimensional plasmonic collimators. *Appl Phys Lett* 2008;93:181101.
- [45] Yu N, Blanchard R, Fan J, Wang QJ, Pflügl C, Diehl L, Edamura T, Yamanishi M, Kan H, Capasso F. Quantum cascade lasers with integrated plasmonic antenna-array collimators. *Opt Express* 2008;16:19447–61.
- [46] Yu N, Aieta F, Genevet P, Kats MA, Gaburro Z, Capasso F. A broadband, background-free quarter-wave plate based on plasmonic metasurfaces. *Nano Lett* 2012;12:6328–33.
- [47] Huang L, Chen X, Mühlenbernd H, Li G, Bai B, Tan Q, Jin G, Zentgraf T, Zhang S. Dispersionless phase discontinuities for controlling light propagation. *Nano Lett* 2012;12:5750–5.
- [48] Zhan Q. Cylindrical vector beams: from mathematical concepts to applications. *Adv Opt Photon* 2009;1:1–57.
- [49] Ghadyani Z, Vartiainen I, Harder I, Iff W, Berger A, Lindlein N, Kuittinen M. Concentric ring metal grating for generating radially polarized light. *Appl Opt* 2011;50:2451–7.
- [50] Pfeiffer C, Emani NK, Shaltout AM, Boltasseva A, Shalaev VM, Grbic A. Efficient light bending with isotropic metamaterial Huygens’ surfaces. *Nano Lett* 2014;14:2491–7.
- [51] Eitan M, Iluz Z, Yifat Y, Boag A, Hanein Y, Scheuer J. Degeneracy breaking of Wood’s anomaly for enhanced refractive index sensing. *ACS Photon* 2015;2:615–21.

- [52] Montelongo Y, Tenorio-Pear JO, Milne WI, Wilkinson TD. Polarization switchable diffraction based on subwavelength plasmonic nanoantennas. *Nano Lett* 2014;14:294–8.
- [53] Farmahini-Farahani M, Mosallaei H. Birefringent reflectarray metasurface for beam engineering in infrared. *Opt Lett* 2013;38:462–4.
- [54] Pors A, Nielsen MG, Eriksen RL, Bozhevolnyi SI. Broadband focusing flat mirrors based on plasmonic gradient metasurfaces. *Nano Lett* 2013;13:829–34.
- [55] Pancharatnam S. Generalized theory of interference and its applications. *Proc Indian Acad Sci A* 1956;44:398–417.
- [56] Berry MV. Quantal phase-factors accompanying adiabatic changes. *Proc R Soc Lond A* 1984;392:45–57.
- [57] Zhan Q, Leger JR. Interferometric measurement of the geometric phase in space-variant polarization manipulations. *Opt Comm* 2002;213:241–5.
- [58] Kang M, Chen J, Wang XL, Wang HT. Twisted vector field from an inhomogeneous and anisotropic metamaterial. *J Opt Soc Am B* 2012;29:572–6.
- [59] Kang M, Feng T, Wang HT, Li J. Wave front engineering from an array of thin aperture antennas. *Opt Exp* 2012;20:15882–90.
- [60] Shitrit N, Bretner I, Gorodetski Y, Kleiner V, Hasman E. Optical spin Hall effects in plasmonic chains. *Nano Lett* 2011;11:2038–42.
- [61] Yifat Y, Iluz Z, Eitan M, Friedler I, Hanein Y, Boag A, Scheuer J. Quantifying the radiation efficiency of nano antennas. *Appl Phys Lett* 2012;100:111113.
- [62] Yifat Y, Iluz Z, Bar-Lev D, Eitan M, Hanein Y, Boag A, Scheuer J. High load sensitivity in wideband infrared dual-Vivaldi nanoantennas. *Opt Lett* 2013;38:205–7.
- [63] Bomzon Z, Kleiner V, Hasman E. Pancharatnam–Berry phase in space-variant polarization-state manipulations with subwavelength gratings. *Opt Lett* 2001;18:1424–6.
- [64] Yirmiyahu Y, Niv A, Biener G, Kleiner V, Hasman E. Vectorial vortex mode transformation for a hollow waveguide using Pancharatnam–Berry phase optical elements. *Opt Lett* 2006;22:3252–4.
- [65] Lin D, Fan P, Hasman E, Brongersma ML. Dielectric gradient metasurface optical elements. *Science* 2014;345:298–302.
- [66] Novotny L, Hecht N. Principles of nano-optics. New York, USA: Cambridge University Press, 2006.
- [67] Love AEH. The integration of the equations of propagation of electric waves. *Philos Trans R Soc A* 1901;68:19–21.
- [68] Schelkunoff SA. Some equivalence theorems of electromagnetics and their application to radiation problems. *Bell Syst Tech J* 1936;15:92–112.
- [69] Evlyukhin AB, Reinhardt C, Seidel A, Luk'yanchuk BS, Chichkov BN. Optical response features of Si-nanoparticle arrays. *Phys Rev B* 2010;82:045404.
- [70] Popa BI, Cummer SA. Compact dielectric particles as a building block for low-loss magnetic metamaterials. *Phys Rev Lett* 2008;100:207401.
- [71] García-Extarri A, Gómez-Medina R, Froufe-Pérez LS, López C, Chantada L, Scheffold F, Aizpurua J, Nieto-Vesperinas M, Sáenz JJ. Strong magnetic response of submicron silicon particles in the infrared. *Opt Express* 2011;19:4815–26.
- [72] Kuznetsov AI, Miroshnichenko AE, Fu YH, Zhang J, Luk'yanchuk B. Magnetic light. *Sci Rep* 2012;2:492.
- [73] Evlyukhin AB, Novikov SM, Zywiets U, Eriksen RL, Reinhardt C, Bozhevolnyi SI, Chichkov BN. Demonstration of magnetic dipole resonances of dielectric nanospheres in the visible region. *Nano Lett* 2012;12:3749–55.
- [74] Shi L, Tuzer TU, Fenollosa R, Meseguer F. A new dielectric metamaterial building block with a strong magnetic response in the sub-1.5-micrometer region: silicon colloid nanocavities. *Adv Mater* 2012;24:5934–8.
- [75] Ginn JC, Brener I, Peters DW, Wendt JR, Stevens JO, Hines PF, Basilio LI, Warne LK, Ihlefeld JF, Clem PG, Sinclair MB. Realizing optical magnetism from dielectric metamaterials. *Phys Rev Lett* 2012;108:097402.
- [76] Kerker M, Wang DS, Giles CL. Electromagnetic scattering by magnetic spheres. *J Opt Soc Am* 1983;73:765–7.
- [77] Bohren CF, Huffman DR. Absorption and scattering of light by small particles. New York: John Wiley & Sons Inc, 1983.
- [78] Fu YH, Kuznetsov AI, Miroshnichenko AE, Yu YF, Luk'yanchuk B. Directional visible light scattering by silicon nanoparticles. *Nat Commun* 2013;4:1527.
- [79] Shi L, Harris JT, Fenollosa R, Rodriguez I, Lu X, Korgel BA, Meseguer F. Monodisperse silicon nanocavities and photonic crystals with magnetic response in the optical region. *Nat Commun* 2013;4:1904.
- [80] Cheng J, Ansari-Oghol-Beig D, Mosallaei H. Wave manipulation with designer dielectric metasurfaces. *Opt Lett* 2014;39:6285–8.
- [81] Staude I, Miroshnichenko AE, Decker M, Fofang NT, Liu S, Gonzales E, Dominguez J, Luk TS, Neshev DN, Brener I, Kivshar Y. Tailoring directional scattering through magnetic and electric resonances in subwavelength silicon nanodisks. *ACS Nano* 2013;7:7824–32.
- [82] Decker M, Staude I, Falkner M, Dominguez J, Neshev DN, Brener I, Pertsch T, Kivshar Y. High-efficiency dielectric Huygens' surfaces. *Adv Opt Mater* 2015;3:813–20.
- [83] Shalaev MI, Sun J, Tsukernik A, Pandey A, Nikolskiy K, Litchinitser NM. High-efficiency all-dielectric metasurfaces for ultracompact beam manipulation in transmission mode. *Nano Lett* 2015;15:6261–6.
- [84] Yu YF, Zhu AY, Paniagua-Domínguez R, Fu YH, Luk'yanchuk B, Kuznetsov AI. High-transmission dielectric metasurface with 2 phase control at visible wavelengths. *Laser Photon Rev* 2015;9:412–8.
- [85] Arbabi A, Briggs RM, Horie Y, Bagheri M, Faraon A. Efficient dielectric metasurface collimating lenses for mid-infrared quantum cascade lasers. *Opt Express* 2015;23:33310–7.
- [86] Lawrence N, Trevino J, Dal Negro L. Aperiodic arrays of active nanopillars for radiation engineering. *J Appl Phys* 2012;111:113101.
- [87] Chong KE, Staude I, James A, Dominguez J, Liu S, Campione S, Subramania GS, Luk TS, Decker M, Neshev DN, Brener I, Kivshar YS. Polarization independent silicon metadevices for efficient optical wavefront control. *Nano Lett* 2015;15:5369–74.
- [88] Yang Y, Wang W, Moitra P, Kravchenko II, Briggs DP, Valentine J. Dielectric meta-reflectarray for broadband linear polarization conversion and optical vortex generation. *Nano Lett* 2014;14:1394–9.
- [89] Arbabi A, Horie Y, Bagheri M, Faraon A. Dielectric metasurfaces for complete control of phase and polarization with subwavelength spatial resolution and high transmission. *Nat Nano* 2015;10:937–43.

- [90] Prodan E, Radloff C, Halas BJ, Nordlander P. A hybridization model for the plasmon response of complex nanostructures. *Science* 2003;302:419–22.
- [91] Stutzman WL, Thiele GA. *Antenna Theory and Design*, 2<sup>nd</sup> ed. New Jersey, USA: Wiley, 1998.
- [92] Hesselting C, Woerdemann M, Hermerschmidt A, Denz C. Controlling ghost traps in holographic optical tweezers. *Opt Lett* 2011;36:3657–9.
- [93] Aieta F, Kats MA, Genevet P, Capasso F. Multiwavelength achromatic metasurfaces by dispersive phase compensation. *Science* 2015;347:1342–5.
- [94] Kalvach A, Szabó Z. Aberration-free flat lens design for a wide range of incident angles. *J Opt Soc Am B* 2016;33:A66–71.
- [95] Shiloh R, Remez R, Arie A. Prospects for electron beam aberration correction using sculpted phase masks. *Ultramicroscopy* 2016;163:69–74.
- [96] Kang S, Joe HE, Kim J, Jeong Y, Min BK, Oh K. Subwavelength plasmonic lens patterned on a composite optical fiber facet for quasi-one-dimensional Bessel beam generation. *Appl Phys Lett* 2011;98:241103.
- [97] Smythe EJ, Dickey MD, Whitesides GM, Capasso F. A technique to transfer metallic nanoscale patterns to small and non-planar surfaces. *ACS Nano* 2009;3:59–65.
- [98] Yua X, Yong D, Zhang H, Li H, Zhang Y, Chan CC, Ho HP, Liu H, Liu D. Plasmonic enhanced fluorescence spectroscopy using side-polished microstructured optical fiber. *Sens Act B* 2011;160:196–201.
- [99] Smythe EJ, Dickey MD, Bao J, Whitesides GM, Capasso F. Optical antenna arrays on a fiber facet for in situ surface-enhanced Raman scattering detection. *Nano Lett* 2009;9:1132–8.
- [100] Lipomi DJ, Martinez RV, Kats MA, Kang SH, Kim P, Aizenberg J, Capasso F, Whitesides GM. Patterning the tips of optical fibers with metallic nanostructures using nanoskiving. *Nano Lett* 2011;11:632–6.
- [101] Lee N, Roh S, Park J. Current status of micro- and nano-structured optical fiber sensors. *Opt Fiber Technol* 2009;15:209–21.
- [102] Yu N, Wang QJ, Kats MA, Fan JA, Khanna SP, Li L, Davies AG, Linfield EH, Capasso F. Designer spoof-surface-plasmon structures collimate terahertz laser beams. *Nat Mater* 2010;9:730–5.
- [103] Yu N, Wang QJ, Kats M, Fan JA, Capasso F, Khanna SP, Li L, Davies AG, Linfield EH. Terahertz plasmonics. *Electron Lett* 2010;46:s52–7.
- [104] Streier W, Law S, Rooney G, Jacobs T, Wasserman D. Strong absorption and selective emission from engineered metals with dielectric coatings. *Opt Express* 2013;21:9113–22.
- [105] Mason JA, Smith S, Wasserman D. Strong absorption and selective thermal emission from a midinfrared metamaterial. *Appl Phys Lett* 2011;98:241105.
- [106] Falcone F, Lopetegi T, Laso MAG, Baena JD, Bonache J, Beruete M, Marqués R, Martín F, Sorolla M. Babinet principle applied to the design of metasurfaces and metamaterials. *Phys Rev Lett* 2004;93:197401.
- [107] Born N, Reuter M, Koch M, Scheller M. High-Q terahertz bandpass filters based on coherently interfering metasurface reflections. *Opt Lett* 2013;38:908–10.
- [108] Jansen C, Al-Naib IAI, Born N, Koch M. Terahertz metasurfaces with high Q-factors. *Appl Phys Lett* 2011;98:051109.
- [109] Jiang NH, Yun S, Lin L, Bossard JA, Werner DH, Mayer TS. Tailoring dispersion for broadband low-loss optical metamaterials using deep-subwavelength inclusions. *Sci Rep* 2013;3:1571.
- [110] Shitrit N, Yulevich I, Maguid E, Ozeri D, Veksler D, Kleiner V, Hasman E. Spin-optical metamaterial route to spin-controlled photonics. *Science* 2013;340:724–6.
- [111] Gorodetski Y, Shitrit N, Bretner I, Kleiner V, Hasman E. Observation of optical spin symmetry breaking in nanoapertures. *Nano Lett* 2009;9:3016–9.
- [112] Segal N, Keren-Zur S, Hendler N, Ellenbogen T. Controlling light with metamaterial-based nonlinear photonic crystals. *Nat Photon* 2015;9:180–4.
- [113] Klein MW, Enkrich C, Wegener M, Linden S. Second-harmonic generation from magnetic metamaterials. *Science* 2006;313:502–4.
- [114] Shadrivov IV, Zharov AA, Kivshar YS. Second-harmonic generation in nonlinear left-handed metamaterials. *J Opt Soc Am B* 2006;23:529–34.
- [115] Husu H, Siikanen R, Mäkitalo J, Lehtolahti J, Laukkanen J, Kuitinen M, Kauranen M. Metamaterials with tailored nonlinear optical response. *Nano Lett* 2012;12:673–7.
- [116] Ciraci C, Poutirina W, Scalora M, Smith DR. Origin of second-harmonic generation enhancement in optical split-ring resonators. *Phys Rev B* 2012;85:201403.
- [117] Kauranen M, Zayats AV. Nonlinear plasmonics. *Nat Photon* 2012;6:737–48.
- [118] Salomon A, Zielinski M, Kolkowski R, Zyss J, Prior Y. Size and shape resonances in second harmonic generation from silver nanocavities. *J Phys Chem C* 2013;117:22377–82.
- [119] Bar-Lev D, Scheuer J. Efficient second harmonic generation using nonlinear substrates patterned by nano-antenna arrays. *Opt Express* 2013;21:29165–78.
- [120] Smith SJ, Purcell EM. Visible light from localized surface charges moving across a grating. *Phys Rev* 1953;92:1069.
- [121] Andriyash IA, Lehe R, Lifschitz A, Thauray C, Rax JM, Krushelnick K, Malka V. An ultracompact X-ray source based on a laser-plasma undulator. *Nat Commun* 2014;5:4736.
- [122] Corde S, Ta Phuoc K, Lambert G, Fitour R, Malka V, Rousse A, Beck A, Lefebvre E. Femtosecond x rays from laser-plasma accelerators. *Rev Mod Phys* 2013;85:1–48.
- [123] Saldin E, Schneidmiller EV, Yurkov MV. *The physics of free electron lasers (advanced texts in physics)*. Berlin Heidelberg New-York: Springer, 2000.
- [124] Plettner T, Lu PP, Byer RL. Proposed few-optical cycle laser-driven particle accelerator structure. *Phys Rev ST Accel Beams* 2006;9:11301.
- [125] Peralta EA, Soong K, England RJ, Colby ER, Wu Z, Montazeri B, McGuinness C, McNeur J, Leedle KJ, Walz D, Sozer EB, Cowan B, Schwartz B, Travish G, Byer RL. Demonstration of electron acceleration in a laser-driven dielectric microstructure. *Nature* 2013;503:91–4.
- [126] Bar-Lev D, Scheuer J. Plasmonic metasurface for efficient ultrashort pulse laser-driven particle acceleration. *Phys Rev ST Accel Beams* 2014;17:121302.
- [127] Sun J, Timurdogan E, Yaacobi A, Hosseini ES, Watts MR. Large-scale nanophotonic phased array. *Nature* 2013;493:195–9.
- [128] Zheludev NI. Obtaining optical properties on demand. *Science* 2015;348:973–4.

- [129] Murray WA, Augu   B, Barnes BL. Sensitivity of localized surface plasmon resonances to bulk and local changes in the optical environment. *J Phys Chem C* 2009;113:5120–5.
- [130] Kats MA, Blanchard R, Genevet P, Yang Z, Qazilbash MM, Basov DN, Ramanathan S, Capasso F. Thermal tuning of mid-infrared plasmonic antenna arrays using a phase change material. *Opt Lett* 2013;38:368–70.
- [131] Ou JY, Plum E, Jiang L, Zheludev NI. Reconfigurable photonic metamaterials. *Nano Lett* 2011;11:2142–4.
- [132] Ou JY, Plum E, Zhang L, Zheludev NI. An electromechanically reconfigurable plasmonic metamaterial operating in the near-infrared. *Nature Nanotech* 2013;8:252–5.
- [133] Wang X, Belyanin AA, Crooker SA, Mittleman DM, Kono J. Interference-induced terahertz transparency in a magneto-plasma in a semiconductor. *Nat Phys* 2010;6:126–30.
- [134] Valente J, Ou JY, Plum E, Youngs IJ, Zheludev NI. A magneto-electrooptical effect in plasmonic nanowire material. *Nat Commun* 2015;6:7021.
- [135] Chen HT, Padilla WJ, Zide JMO, Gossard AC, Taylor AJ, Averitt RD. Active terahertz metamaterial devices. *Nature* 2006;444:597–600.
- [136] Ju L, Geng B, Horng J, Girit C, Martin M, Hao Z, Bechtel HA, Liang X, Zettl A, Shen YR, Wang F. Graphene plasmonics for tunable terahertz metamaterials. *Nat Nano* 2011;6:630–4.
- [137] Vakil A, Engheta N. Transformation optics using graphene. *Science* 2011;332:1291–4.
- [138] Fallahi A., Perruisseau-Carrier J. Design of tunable biperiodic graphene metasurfaces. *Phys Rev B* 2012;86:195408.
- [139] Carrasco E, Tamagnone M, Perruisseau-Carrier J. Tunable graphene reflective cells for THz reflectarrays and generalized law of reflection. *Appl Phys Lett* 2013;102:104103.
- [140] Yao Y, Kats MA, Genevet P, Yu N, Song Y, Kong J, Capasso F. Broad electrical tuning of graphene-loaded plasmonic antennas. *Nano Lett* 2013;13:1257–64.
- [141] Li Z, Yu N. Modulation of mid-infrared light using graphene-metal plasmonic antennas. *Appl Phys Lett* 2013;102:131108.
- [142] Fang Z, Thongrattanasiri S, Schlather A, Liu Z, Ma L, Wang Y, Ajayan PM, Nordlander P, Halas NJ, Garc  a de Abajo FJ. Gated tunability and hybridization of localized plasmons in nano-structured graphene. *ACS Nano* 2013;7:2388–95.
- [143] Ren X, Wei EI, Choy WCH. Tuning optical responses of metallic dipole nanoantenna using graphene. *Opt Express* 2013;21:31824–9.
- [144] Huang C, Bouhelier A, Berthelot J, des-Francis GC, Finot E, Weeber JC, Dereux A, Kostcheev S, Baudrion AL, Plain J, Bachelot R, Royer P, Wiederrecht GP. External control of the scattering properties of a single optical nanoantenna. *Appl Phys Lett* 2010;96:143116.
- [145] Gu J, Singh R, Liu X, Zhang X, Ma Y, Zhang S, Maier SA, Tian Z, Azad AK, Chen HT, Taylor AJ, Han J, Zhang W. Active control of electromagnetically induced transparency analogue in terahertz metamaterials. *Nat Commun* 2012;3:1151.
- [146] Shadrivov IV, Kapitanova PV, Maslovski SI, Kivshar YS. Metamaterials controlled with light. *Phys Rev Lett* 2012;109:083902.
- [147] Pryce IM, Aydin K, Kelaita YA, Briggs RM, Atwater HA. Highly strained compliant optical metamaterials with large frequency tunability. *Nano Lett* 2010;10:4222–7.
- [148] Lapine M, Shadrivov IV, Powell DA, Kivshar YS. Magnetoelastic metamaterials. *Nat Mater* 2012;11:30–3.
- [149] Tao H, Strikwerda AC, Fan K, Padilla WJ, Zhang X, Averitt RD. Reconfigurable terahertz metamaterials. *Phys Rev Lett* 2009;103:147401.
- [150] Abb M, Albella P, Aizpurua J, Muskens OL. All-optical control of a single plasmonic nanoantenna-ITO hybrid. *Nano Lett* 2011;11:2457–63.
- [151] Kats MA, Sharma D, Lin J, Genevet P, Blanchard R, Yang Z, Qazilbash MM, Basov DN, Ramanathan S, Capasso F. Ultra-thin perfect absorber employing a tunable phase change material. *Appl Phys Lett* 2012;101:221101.
- [152] Kaplan G, Aydin K, Scheuer J. Dynamically controlled plasmonic nano-antenna phased array utilizing vanadium dioxide. *Opt Mater Express* 2014;5:2513–24.
- [153] Qazilbash M, Brehm M, Chae BG, Ho PC, Andreev GO, Kim BJ, Yun SJ, Balatsky AV, Maple MB, Keilmann F, Kim HT, Basov DN. Mott transition in VO<sub>2</sub> revealed by infrared spectroscopy and nano-imaging. *Science* 2007;318:1750–3.
- [154] Gholipour B, Zhang J, Macdonald KF, Hewak DW, Zheludev NI. An all-optical, non-volatile, bidirectional, phase-change meta-switch. *Adv Mater* 2013;25:3050–4.
- [155] Driscoll T, Kim HT, Chae BG, Kim BJ, Lee YW, Marie Jokerst N, Palit S, Smith DR, Di Ventra M, Basov DN. Memory metamaterials. *Science* 2009;325:1518–21.
- [156] Michel AKU, Chigrin DN, Ma  TW, Sch  nauer K, Salinga M, Wuttig M, Taubner T. Using low-loss phase-change materials for mid-infrared antenna resonance tuning. *Nano Lett* 2013;13:3470–5.
- [157] Dicken MJ, Aydin K, Pryce IM, Sweatlock LA, Boyd EM, Wala-valkar S, Ma J, Atwater HA. Frequency tunable near-infrared metamaterials based on VO<sub>2</sub> phase transition. *Opt Express* 2009;17:18330–9.
- [158] Papaioannou M, Plum E, Valente J, Rogers E, Zheludev NI. Two-dimensional control of light with light on metasurfaces. *Light Sci Appl* 2016;5:e16070.
- [159] Wang Q, Rogers ETF, Gholipour B, Wang CM, Yuan G, Teng J, Zheludev NI. Optically reconfigurable metasurfaces and photonic devices based on phase change materials. *Nat Photon* 2016;10:60–5.